RESEARCH ARTICLE
doi: 10.2306/scienceasia1513-1874.2022.048

ScienceAsia 48 (2022): **278–286**

Physicochemical and biological activities of the gamma-irradiated blended fibroin/aloe gel film

Preeyawass Phimnuan[a], **Saran Worasakwutiphong**[b], **Anuphan Sittichokechaiwut**[c], **Francois Grandmottet**[d], **Wongnapa Nakyai**[e], **Kunlathida Luangpraditkun**[a], **Céline Viennet**[f], **Jarupa Viyoch**[a,*]

[a] Department of Pharmaceutical Technology, Faculty of Pharmaceutical Sciences and Center of Excellence for Innovation in Chemistry, Naresuan University, Phitsanulok 65000 Thailand
[b] Division Plastic and Reconstructive Surgery, Department of Surgery, Faculty of Medicine, Naresuan University, Phitsanulok 65000 Thailand
[c] Department of Preventive Dentistry, Faculty of Dentistry, Naresuan University, Phitsanulok 65000 Thailand
[d] Department of Biochemistry, Faculty of Medical Science, Naresuan University, Phitsanulok 65000 Thailand
[e] Department of Chemistry, Faculty of Science, Ramkhamhaeng University, Bangkok 10240 Thailand
[f] UMR 1098 RIGHT INSERM EFS BFC, University of Bourgogne Franche-Comté, Besançon, 25000 France

*Corresponding author, e-mail: jarupav@nu.ac.th

Received 12 Jul 2021, Accepted 17 Dec 2021
Available online 28 Feb 2022

ABSTRACT: The physicochemical and biological properties of the blended fibroin/aloe gel film as a wound dressing were investigated to support the wound healing efficacy of the film described in our previous study. In the current study, protein content, molecular weight pattern, and chemical characteristics of the silk fibroin and the aloe gel extracts were analyzed. The two extracts were then dissolved in lactic acid solution and casted to obtain the blended fibroin/aloe gel film. We found that gamma irradiation did not affect any physicochemical properties of the film, i.e., the irradiated and the non-sterilized films had similar physical appearance, surface morphology, mechanical properties, and chemical characteristics. On normal human fibroblast cultures, the film induced non-cytotoxicity and stimulated the expression of vascular epidermal growth factor. The film-treated cells were shown to proliferate by shifting from G_0/G_1 phase ($76.26 \pm 0.72\%$) to S phase ($7.19 \pm 0.23\%$) and G_2/M phase ($16.09 \pm 0.58\%$) which are higher than the untreated cells. The film-treated cells provided a completely healed scratch at 36 h after scratch creation, while the created scratch of the untreated cells was not healed, indicating that the biological activity of the film enhanced the proliferation and the migration of fibroblast cells. We speculated that the prepared film might be able to use as wound dressing for the diabetic foot ulcer.

KEYWORDS: silk fibroin, aloe gel, gamma-irradiation, wound dressing

INTRODUCTION

Diabetic foot ulcer (DFU), defined as a foot affected by ulceration, is one of the most serious complications of diabetes mellitus (DM) [1]. Several artificial DM polymeric materials have been developed for application as wound dressings. Besides, the utilization of natural biomaterials based on silk fibroin and aloe gel extracts, shown to have wound healing properties *in vitro*, *in vivo*, and clinical trial, has also been reported [2, 3].

Silk fibroin, from the cocoons of *Bombyx mori* silk worm, has been highlighted for various applications in the biomedical field due to its superior mechanical properties, controllable biodegradability, hemostatic properties, non-cytotoxicity, and non-inflammatory characteristics [4, 5]. Silk fibroin also exhibits exceptional compatibility with a variety of cells and tissues [2]. Because of its properties on enhancing the migration and proliferation of various cells, silk fibroin has been considered as a potential biomaterial to be used as wound dressings with many formulations.

Aloe vera has been traditionally used in diverse cultures for its therapeutic properties including rejuvenation, dermatologic conditions, and especially wound healing properties [6, 7]. Many chemical compounds are found in the *Aloe vera* leaf, including acetylated mannans, polymannans, anthraquinone C-glycosides, anthrones, anthraquinones, and lectins [8]. Although it has been widely used as a folk treatment, few scientific studies have been reported on the incorporation of *Aloe vera* with silk fibroin and the effects of the product' biological properties in wound healing [9].

Our previous studies showed that a film prepared from a blend of silk fibroin and aloe gel extracts significantly accelerated the wound healing rate in streptozotocin-induced diabetic rats [2]. In addition, the film rapidly attenuated the healing time and the wound size in 5 DFU patients with complete healing within 4 weeks. In the current study, a blended fibroin/aloe gel film was prepared and sterilized by gamma irradiation. Then, the physicochemical and biological properties of the film were analyzed, and the effects on the wound healing efficacy of the film were determined.

For the biological effects, we focused on the expression of growth factor, proliferation, and migra-

tion of skin fibroblast activities associated with wound granulation and subsequent wound closure. We also expected to demonstrate that the physicochemical properties of the sterilized film would not be altered by gamma irradiation process, and that the biological activities of gamma-irradiated film would enhance wound healing.

MATERIALS AND METHODS

Materials

Yellow silkworm cocoons (*Bombyx Mori*, Nang-Laai strain) were contributed by the Queen Sirikit Sericulture Center, Chiang Mai Province, Thailand. *Aloe vera* was cultured and collected from Phitsanulok Province, Thailand. Chemicals/materials were purchased from different companies: calcium chloride, sodium hydroxide, and ammonium sulfate from RCI Labscan, Bangkok, Thailand; lactic acid solution (88%), sulfuric acid, and lipopolysaccharide (LPS) from Sigma-Aldrich Chemie GmbH, Steinheim, Germany; dialysis membrane standard RC tubing (MWCO: 6–8 kDa) from Spectrum Laboratories, Inc., California, USA; detergent compatible (DC) protein assay kit from BIO-RAD Laboratories, Philadelphia, USA; phenol from AppliChem GmbH, Darmstadt, Germany; Modified Eagle's Medium (DMEM), fetal bovine serum (FBS), and 0.25% trypsin/0.01M EDTA from Sigma-Aldrich Co., Missouri, USA; penicillin/streptomycin solution (10 000 U/ml) and amphotericin B (250 µg/ml) from Gibco, Invitrogen, Massachusetts, USA; cell proliferation kit II (2,3-bis (2-methoxy-4-nitro-5-sulphophenyl)-5-[(phenylamino)carbonyl]-2H-tetrazoliumhydroxide, XTT) from Roche Diagnostics GmbH, Mannheim, Germany; Mueller Hinton Agar from HiMedia, Mumbai, India; and Muse™ Cell Cycle Assay Kit SDS from MERCK, Darmstadt, Germany.

Preparation and characteristic determination of the fibroin extract

The extraction of silk fibroin was performed according to the method described our previous study with some modifications [2]. Briefly, small pieces of silkworm cocoons were treated with hot deionized (DI) water at 85–90 °C for 2 h followed by 25 mM NaOH at 70 °C for 30 min to remove silk gum protein. The degummed fibers were washed with DI water and dried at 45 °C overnight. The dried samples were dissolved in 3 M $CaCl_2$ solution (1 g of samples to 60 ml of $CaCl_2$) at 85–90 °C for 4–6 h. The resulting solution was filtered and dialyzed against 15 MΩ water using dialysis membrane standard RC tubing (MWCO 6–8 kDa) at 23 ± 2 °C for 2 days, with changes of water every 4–6 h, until salts were completely removed. The desalted solution was then centrifuged at 8000 rpm at 4 °C for 15 min. Finally, the supernatants were collected and lyophilized, and the lyophilized fibroin extract was kept in the desiccator at 25 ± 2 °C until further use. The protein content and the molecular weight pattern of the fibroin extract were determined using DC protein assay kit and sodium dodecyl sulfate polyacrylamide gel electrophoresis (SDS-PAGE) method, respectively [2]. The chemical characteristics of the extract were analyzed using Fourier transform infrared spectroscopy (FTIR spectrometer, Spectrum GX series, USA) [2].

Preparation and characteristic determination of the *Aloe vera* gel extract

The extract of *Aloe vera* gel was prepared according to the method described our previous study with some modifications [2]. Briefly, the colorless gel part was collected, homogenized, and centrifuged at 12 000 rpm at 4 °C for 15 min. The supernatant was collected and precipitated by adding $(NH_4)_2SO_4$ to get 55% (w/v) of $(NH_4)_2SO_4$. The resulting precipitates were isolated, dissolved in DI water. The obtained solution was dialyzed against 15 MΩ water using dialysis membrane standard RC tubing (MWCO 6–8 kDa) at 23 ± 2 °C for 1 day with changes of water every 4–6 h. The desalted solution was lyophilized, and the lyophilized aloe gel extract was kept in the desiccator at 25 ± 2 °C until further use. The protein content and the molecular weight pattern of the extract were determined by DC protein assay kit and SDS-PAGE, respectively. Functional groups of the extract were determined using FTIR spectrometry [2].

Preparation and characteristic determination of the blended fibroin/aloe gel film

The blended fibroin/aloe gel film was prepared by casting method described in our previous study with some modifications [2]. 540 mg of the fibroin extract and 15 mg of the aloe gel extract were separately dissolved for 1 h in aqueous solution (with maintained pH 4.0 ± 0.2 using lactic acid) to a final volume of 15 ml. The mixture solution was then filtered and subsequently cast in a square-shaped silicone mold (6 cm × 6 cm) under a dust-free condition and a maintained temperature of 47 ± 2 °C. The ratio of the fibroin extract and the aloe gel extract in the film (36 cm^2) was 97.3% to 2.7% by weight. The physicochemical characteristics of the films were done as follows; (1) scanning electron microscopy (SEM, DAX®, LEO1455VP, New Jersey, USA) for surface morphology observation; (2) mechanical texture analysis (TA.XT Plus, Stable Micro Systems, Ltd, Godalming, UK) including determination of tensile strength and elongation at break; and (3) Fourier transform infrared spectroscopy (FTIR) for chemical characteristics determination. The film was sterilized by gamma irradiation technique (facilitated by Thai Adhesive Tapes Industry Co., Ltd, Bangkok, Thailand), and the sterility of the irradiated film was confirmed by observing the appearance of bacteria

growth using the agar plate culture technique [10].

Determination of biological activities of the blended fibroin/aloe gel film

Cytocompatibility and expression of growth factor by skin fibroblast cells

Normal human dermal fibroblast (NHDF) cells (Lot no. C-12302, Promocell, Eppelheim, Germany) (1×10^5 cells/well, passage number 6) were seeded in a 24-well plate, cultured in DMEM containing 10% FBS, and incubated at 37 °CC in a humidified 5% CO_2 atmosphere for 24 h. The incubated medium was then replaced with serum-free medium. The sterilized films were cut into pieces in a circular shape (6 mm in diameter and 4.56 mg in weight) and placed into trans-well inserts which were, then, put into individual wells of the 24-well plate containing fibroblast cells and incubated for 24 h. After the incubation, the trans-well inserts were removed from the 24-well plate, and the incubated serum-free medium was then discarded and replaced with 250 µl of new serum-free medium plus XTT reagent. The seeded cells were further incubated for 4 h, and the supernatant was then collected for absorbance measurement at 490 nm using microplate reader (Eon™, BioTek instrument, Vermont, USA). The optical density of the control (untreated cells) was adjusted to 100%, and the cell viability was thus shown in percentage. The experiment was performed in triplicates.

Expression of vascular epidermal growth factor (VEGF) was qualitatively determined using the Anti-VEGFA antibody (ab39250, Abcam, Massachusetts, USA). In brief, film extracts were prepared by incubating 1×1 cm^2 sterilized films in 1 ml of DMEM serum-free and incubated at 37 °C in 5% CO_2 incubator for 24 h. NHDF cells (2×10^5 cells/well, passage number 11) were seeded in a cell culture slide with DMEM containing 10% FBS and incubated at 37 °C in a humidified 5% CO_2 atmosphere for 24 h. The cultured medium was then replaced with the film extracts and incubated for 24 h. Subsequently, cells were fixed with 4% paraformaldehyde in PBS for 10 min at room temperature, permeabilized by 0.1% Triton-X 100 at room temperature for 10 min, and washed 3 times with PBS for 5 min. Cells were then incubated with 1% BSA, 22.52 mg/ml glycine in PBST to block unspecific binding of antibodies. At 30 min later, they were incubated with Anti-VEGFA antibody (diluted in 1% BSA in PBST) in a humidified chamber at 4 °C overnight. After washes with PBS for 3 min (5 times), cells were then incubated with Alexa Fluor®488 conjugated secondary antibody (diluted in 1% BSA in PBST) at room temperature for 1 h in the dark. The secondary antibody solution was discarded, and the cells were washed with PBS for 3 min (5 times). After the washes, the cells were incubated with 100 µl of DAPI (DNA stain) for 1 min and rinsed with PBS for 3 min (5 times). Finally, the cells were mounted with anti-fade mounting solution and observed under Laser confocal microscope (A1 HD25/A1R HD25, Nikon®, Tokyo, Japan).

Cell cycle

NHDF cells (1×10^5 cells/well, passage number 6) were seeded in a 24-well plate and incubated at 37 °C in 5% CO_2 incubator for 24 h. The medium was then replaced by DMEM serum-free. Trans-well inserts containing 6 mm diameter sterilized films were put into a 24-well plate with the adherent fibroblasts and incubated for 24 h. After the incubation, cells were trypsinized using 0.25% trypsin/0.01 M EDTA. Cell suspensions (2×10^5 cells/ml) were centrifuged, and the cell pellet was then washed with PBS (pH 7.4) and fixed with 70% EtOH for 3 h. After the wash, cells were stained with 150 µl of Muse™ Cell Cycle Assay Kit reagent at room temperature for 30 min (protected from light). Cell cycle was then analyzed by flow cytometry. The percentages of total cells for the cell cycle phases (G_0/G_1, S, and G_2/M) of the control (untreated cells) and the film-treated sample were calculated. The experiment was done in 3 replicates.

Migration of skin fibroblasts

The skin fibroblast migration was studied using the scratch assay, which is typically utilized to quantify the migration of cells on two-dimensional (2-D) surfaces over time, following a modified method described in [11, 12]. NHDF cells (1×10^5 cells/well, passage number 7) were seeded in a 24-well plate and incubated at 37 °C in 5% CO_2 incubator for 48 h, during which cells had grown to confluency in a monolayer. A scratch was then made with a pipette tip by creating an incision-like gap in the confluent monolayer of the fibroblasts in each well. The fibroblast scratches were washed twice with sterilized PBS (pH 7.4) followed by adding 800 µl of DMEM serum-free into each well. The trans-well inserts containing the sterilized films (circular shape, 6 mm in diameter) were put into the 24-well plate with fibroblast scratches, and the plate was further incubated at 37 °C in 5% CO_2 incubator for 36 h. The scratched gaps were photographed immediately after scratching at defined time points (0, 12, 24, and 36 h). At 36 h, cell migration was observed as a completed closure of the scratched gaps under an inverted microscope [13]. The experiment was done in three replicates.

Statistical analysis

All values were expressed as mean ± SD. The student's unpaired *t*-test was used to compare between the control and the sample. $p < 0.01$ was considered significant difference.

RESULTS

Characteristics of the fibroin extract

The lyophilized fibroin extract prepared from silkworm cocoons (Nang-Laai strain) presented yellowish cotton-like characteristics. One gram of silk cocoons yielded 0.58 g (58% w/w) of the extract. A DC protein assay showed a protein content of 97.43 ± 0.44% w/w of the extract. Infrared spectra obtained using FTIR spectroscopy showed the frequency peaks at 1634 (amide I), 1513 (amide II), and 1232 (amide III) cm^{-1} (Fig. 1A). The molecular weight pattern of the extract, as shown in Fig. 1B, indicated a specific band of L-chain at approximately 25 kDa and a smear band of H-chain in the range of 30 to 245 kDa.

Characteristics of the aloe gel extract

The lyophilized extract of the *Aloe vera* gel showed white cotton-like characteristics, and 100 g of the gel produced 6 g (0.06% w/w) of the extract. The protein content in the extract was 6.86 ± 1.15% w/w of the extract. Fig. 2A shows the IR spectra of the aloe gel extract indicating peak at 1731 (*O*-acetyl ester), 1238 (*O*-acetyl ester), 1059 (glucan units), 955 (pyranoside ring), and 807 (mannose) cm^{-1}. The molecular weight pattern of the extract showed a clear band at approximately 14 and 35 kDa (Fig. 2B).

Characteristics of the blended fibroin/aloe gel extract

The physical appearance of the prepared film was flexible, translucent, and yellowish with uniform thickness of 50 μm. The SEM images showed a non-porous morphology on the surface of the non-sterilized (Fig. 3A1) as well as sterilized film (Fig. 3A2). For the mechanical properties, the non-sterilized film provided the breaking force and percentage of elongation at break at 6.038 ± 0.746 N and 1.147 ± 0.119%, respectively, which are not significantly different ($p > 0.5$) to the sterilized film (6.26 ± 0.44 N for the breaking force and 1.20 ± 0.07% for percent elongation at break). The FTIR spectroscopy presented infrared spectra of the non-sterilized and sterilized film at 1633 and 1634 (amide I), 1514 and 1513 (amide II), 1231 and 1228 (amide III), 1055 and 1057 (glucan units), 1013 and 1013 (pyranoside ring), 826 and 828 (mannose), respectively, as shown in Fig. 3(B1,B2). Focusing on the sterility test using agar plate culture, the sterilized film showed no colonies of microbes or bacteria growth (Fig. 3C).

Biological activities of the blended fibroin/aloe gel film

For the cytocompatibility of the fibroin/aloe gel film, the viability percentage of the treated NHDF cells was 145.95 ± 1.86, which is significantly higher than the control's (100 ± 5.34) ($p < 0.01$) (Fig. 4A). In the immunofluorescence experiment, the film significantly stimulated the expression of VEGF. Compared with the control, the number and the size/shape of the treated cells were increased (Fig. 4B). In comparison to the control, the treated cells showed a decrease in the percentage of total cells in the G_0/G_1 phase; on the other hand, increases in the percentages of total cells of 7.19 ± 0.23% and 16.09 ± 0.58% were found in the S and the G_2/M phases, respectively, which were higher than those of the untreated cells (2.53 ± 0.92 and 4.67 ± 1.61%, respectively) (Fig. 5). Fig. 6 shows the result of cell migration, measured as the closure of the scratch gap at various times, indicating that at 36 h after scratch creation, the treated cells provided a completely healed scratch, while the scratch of the untreated cells was not healed.

DISCUSSION

In this study, Nang-Laai strain cocoons provided the percentage of yield and the protein content of the fibroin extract corresponding to our previous report [2]. The presence of amides I, II, and III and the random coil groups in the FTIR spectrum confirmed that the extract structure consists of water-soluble random coil conformation [14]. The appearance of the smeared band in the analysis of protein, using SDS-PAGE technique, might be a consequence of the degradation of the heavy (H) chain (325–350 kDa) of silk fibroin protein during the extraction process. The clear band at the range of 17–25 kDa is related to the light (L) chain of fibroin [15].

The percentage of yield and the protein content of the aloe gel extract were similar to our previous findings [2]. The FTIR spectrum showed the presence of functional groups, including glucan units, pyranoside, and mannose relating to anti-inflammatory and healing activities of the aloe gel extract [16, 17]. The SDS-PAGE molecular weight pattern was observed with two clear bands of mannose-binding lectin at approximately 14 and 35 kDa, also indicating the activities of anti-inflammatory [18], hemagglutinating, and mitogenic activities [19] of the extract.

In our current study, the fibroin/aloe gel film was sterilized by gamma irradiation which is one of the most common sterilization methods for health care products including wound dressing [20] and temperature-sensitive materials [21]. However, some studies indicated the adverse effects on molecular mechanisms involving gamma rays-induced cell damages [22], microorganisms resistance [23], and structural changes in medical devices made of polymer [24]. For these reasons, the physical characteristics, chemical, and sterility of the gamma-irradiated film were determined in the present study. The results showed that gamma irradiation efficiently killed the microorganisms on the film; the physicochemical properties of the film were not affected; i.e. its physical appearance, surface morphology, mechanical properties, and chem-

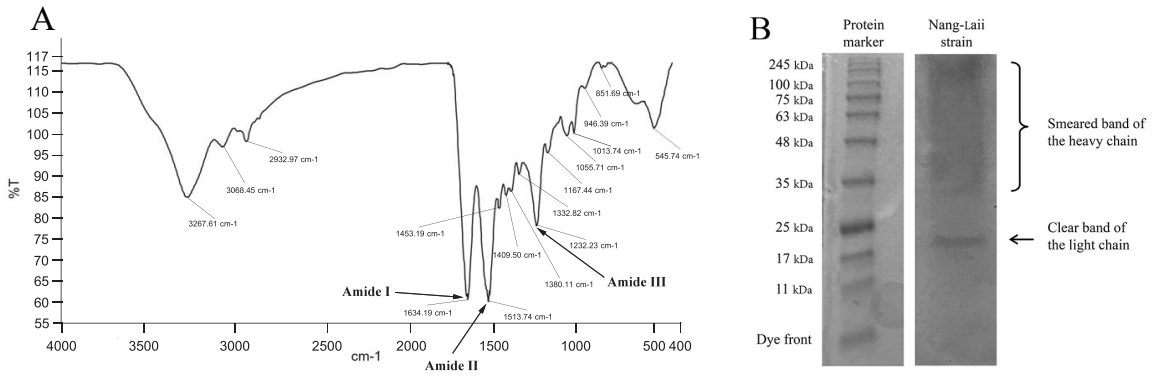

Fig. 1 (A) Infrared spectrum and (B) molecular weight pattern of the fibroin extract prepared from yellow silkworm cocoons (Nang-Laai strain).

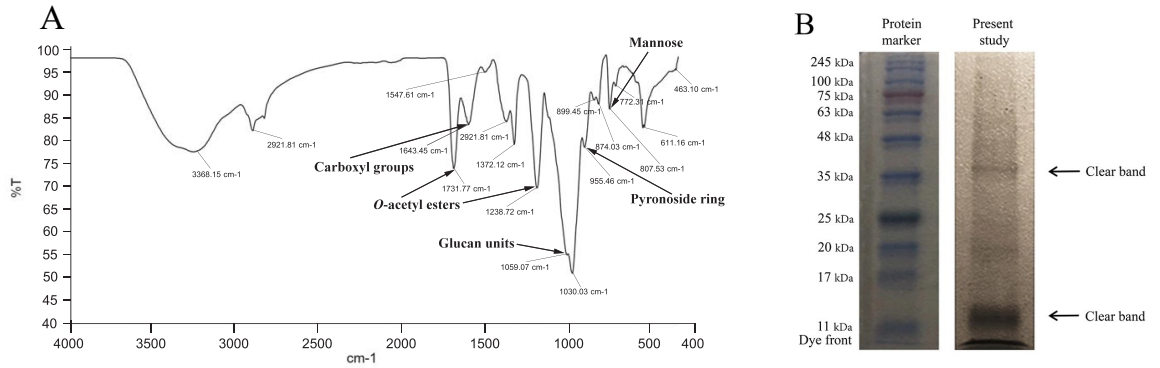

Fig. 2 (A) Infrared spectrum and (B) molecular weight pattern of the aloe gel extract prepared from the gel part of *Aloe vera* leaves.

ical characteristics remained unchanged.

Results from our previous study showed that the fibroin/aloe gel film exerted potential healing effects, *in vitro* and *in vivo*, and promoted wound closure by 7 days compared with the untreated cells in streptozotocin-induced diabetic rats [2]. In a preliminary clinical study, the developed film accelerated the healing rate in 5 DFU patients within 4 weeks. However, in the current study, we sought to emphasize the biological activities associated with healing property to support the efficacy of the film sterilized by gamma irradiation. The cytotoxicity results showed that the sterilized film did not affect the cell viability and morphology. An XTT assay demonstrated that the percentage of cell viability relating to the number of cells had a higher OD value, implying a higher proliferation rate. VEGF can be considered as a key angiogenesis regulator secreted by fibroblasts. It is also one of the most essential mediators associated with the wound healing process because it improves the survival, the proliferation, and the migration of endothelial cells [25, 26]. The results on the expression of VEGF indicated that the sterilized film did not induce any adverse effect, but stimulated an increase in cell number, or the expression of VEGF, indicating the improvement of cell attachment and proliferation as well as the growth factor expression by the primary skin fibroblasts seeded on the film [2]. There have been many studies supporting the potential of the silk fibroin and aloe gel extracts on the acceleration of cell proliferation and cell migration in the wound healing process [2, 27, 28]. To determine the essential role of the fibroin/aloe gel film in the migration and the proliferation of fibroblast cells on the wound healing process, we further performed the flow cytometry and the scratch assay.

Focusing on cell proliferation relating to the cell cycle, which is the complex and orderly cellular process through specific phases during the replication of DNA into two daughter cells, our data revealed that the film-treated cells shifted from G_0/G_1 phase to S phase and then G_2/M phase. Hence, the film promoted the cells to enter into the S and G_2/M phases, which are essential stages for cell mitosis and cell growth, respectively [29]. Besides, Wei et al [30] showed that an acemannan consisting of *Aloe vera* can stimulate cell proliferation by influencing the cyclin-dependent cell cycle through translational regulation of cyclin D1,

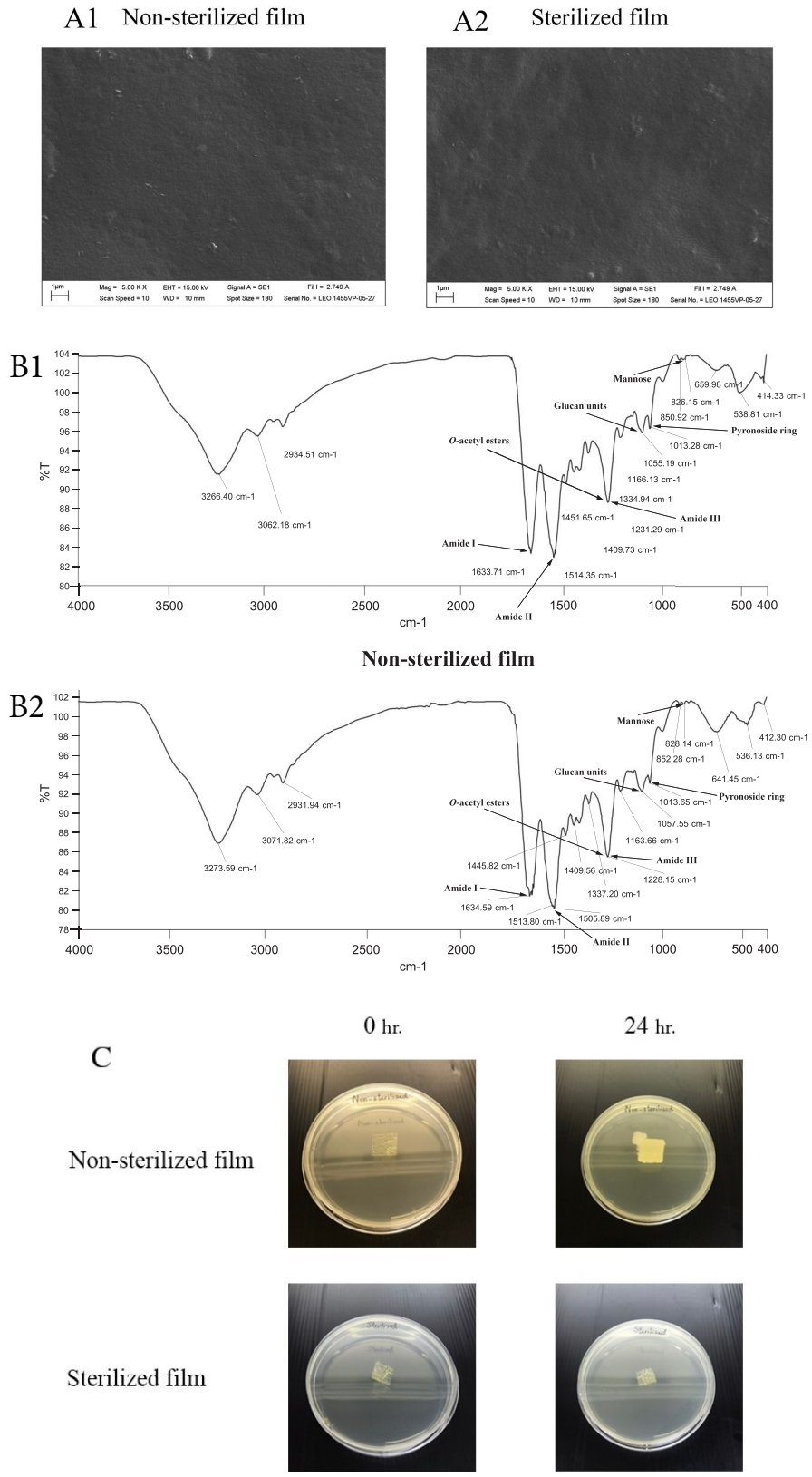

Fig. 3 (A1) SEM images of surface photomicrographs of the non-sterilized film and (A2) the sterilized film; (B1) infrared spectra of the non-sterilized film and (B2) the sterilized film; and (C) sterility test of the non-sterilized and the sterilized films after incubation for 24 h.

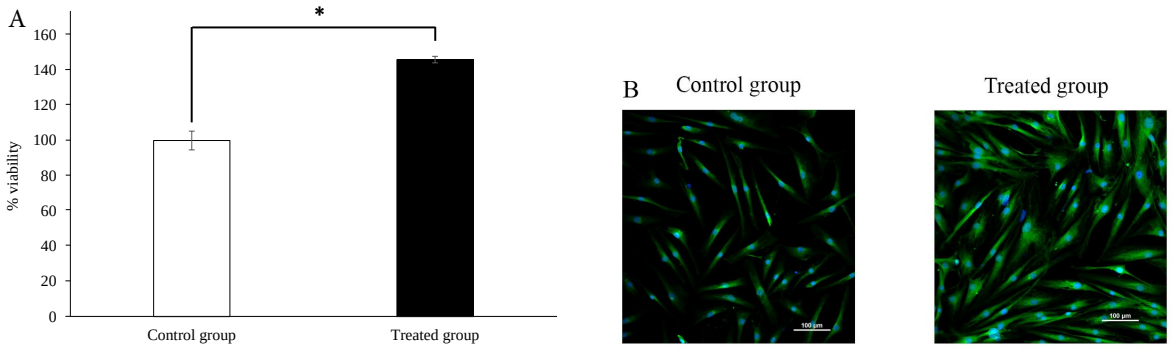

Fig. 4 (A) Viability of NHDF cells treated with the blended fibroin/aloe gel film for 24 h. Data are expressed as percentage of the control (untreated cells), and each column represents mean ± S.D. of triplicate study; * $p < 0.01$. (B) Immunofluorescence for VEGF expression of the control (untreated NHDF cells) and the treated cells at 20 × magnification.

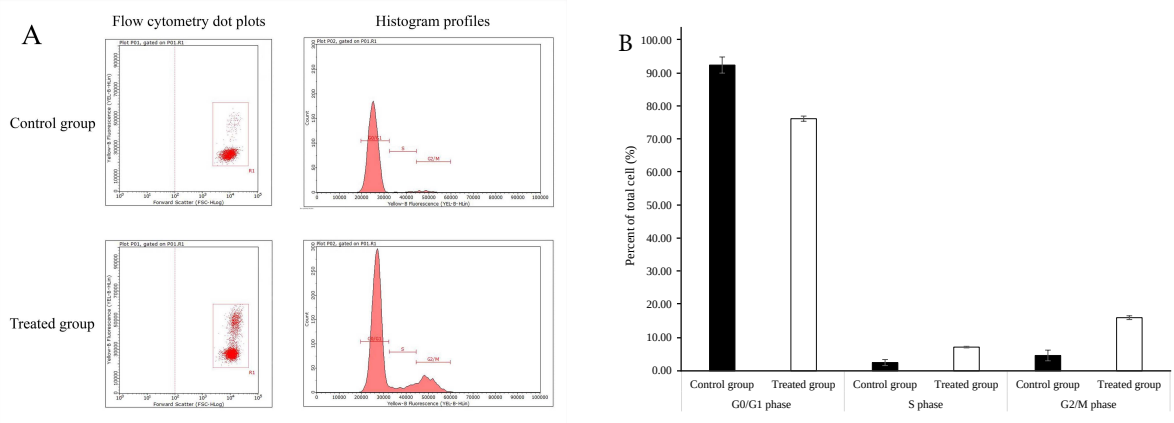

Fig. 5 Cell cycle phases of NHDF cells treated with the blended fibroin/aloe gel film for 24 h compared with the control (untreated cells). The figure shows the examples of cell cycle distribution in: (A) dot plots and histogram profiles; (B) percentage of the total cell. Each column represents mean ± S.D. of triplicate study.

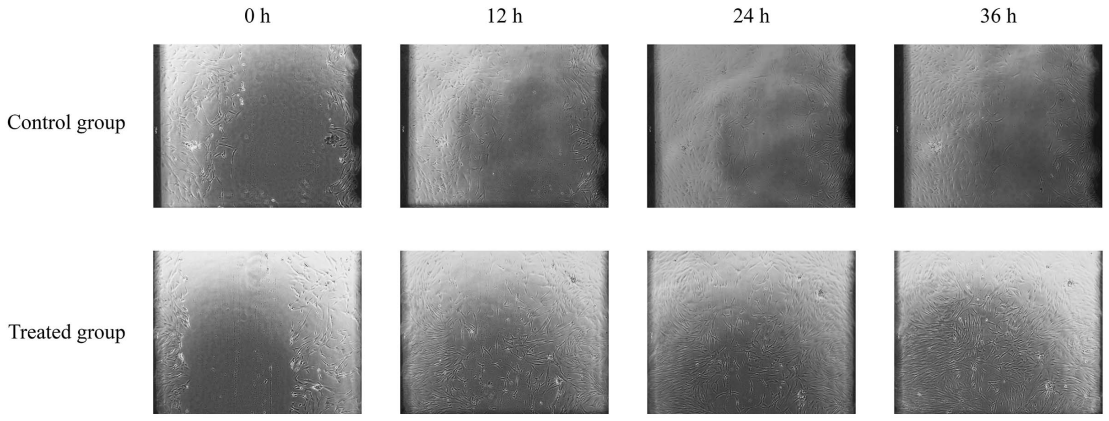

Fig. 6 Cell migration of NHDF cells treated with the blended fibroin/aloe gel film at 0, 12, 24, and 36 h compared with the control (untreated cells) at 10x magnification.

which is the main alteration attributed to the transition of G_1 phase to S phase.

Furthermore, it was found that the fibroin/aloe gel film exerted a beneficial effect by promoting the migration of fibroblasts and, thereby, stimulating wound closure [31]. Additionally, cell proliferation and cell migration are correlated in the cell cycle, particularly in mitosis phase (M phase), associated with the cell division process when duplicated DNA and cytoplasm were divided to create two identical cells [32]. Cell migration can be also correlated to cytoskeletal reorganization and focal adhesion receptors [33]. Interestingly, cell proliferation result described above showed that the highest percentage of total cells in the fibroin/aloe gel film treated cells was found accumulated in the G_2/M phase, implying the promotion of cell differentiation and cell migration processes by the treated cells. The result was consistent with several prior studies reporting that natural compounds promoted G_2/M phase and fibroblast migration [34, 35].

The limitation of this study due to the use of normal fibroblast cells should be noted. In our previous study, the activities of the fibroin/aloe gel film were evaluated in the streptozotocin-induced diabetic rat and the diabetic fibroblast cells related to the DFU patients [2]. In general, the growth factor functions of the diabetic fibroblast cells are impaired leading to the delayed cell proliferation and cell migration when compared with the normal fibroblast cells [36, 37]. However, the presence of functional groups in the fibroin/aloe gel film, including amides (I, II, III), glucan units, pyranoside ring, and mannose, may enhance the proliferation and the migration of cells, leading to wound healing improvement in the diabetic foot ulcers. Nevertheless, further studies on the expression of growth factors and transcription factors of the film in biomolecular level should be performed using human diabetic dermal fibroblast cells to investigate its wound healing efficacy.

CONCLUSION

The physicochemical and biological activities of gamma-irradiated fibroin/aloe gel film were determined to support the wound healing efficacy reported in our previous study. The gamma irradiation was found to have no effects on the film's physicochemical properties (physical appearance, surface morphology, mechanical properties, and chemical characteristics). For biological activities, the blended fibroin/aloe gel film enhanced the proliferation and the migration of the fibroblast cells and, thereby, might be able to help in stimulating the DFU wound healing process.

Acknowledgements: We would like to thank Naresuan University for financial support for graduate student. We also thank the Center of Excellence for Innovation in Chemistry (PERCH-CIC), Office of the Higher Education Commission and the Faculty of Pharmaceutical Sciences, Naresuan University for facility supports. We wish to thank Mr. Roy I. Morien of the Naresuan University Graduate School for his efforts in editing the English grammar and expression in this paper.

REFERENCES

1. Alexiadou K, Doupis J (2012) Management of diabetic foot ulcers. *Diabetes ther* **3**, ID 4.
2. Inpanya P, Faikrua A, Ounaroon A, Sittichokechaiwut, Viyoch J (2012) Effects of the blended fibroin/aloe gel film on wound healing in streptozotocin-induced diabetic rats. *Biomed Mater* **7**, ID 035008.
3. Zhang W, Chen L, Chen J, Wang L, Gui X, Ran J, Xu G, Zhao H, et al (2017) Silk fibroin biomaterial shows safe and effective wound healing in animal models and a randomized controlled clinical trial. *Adv Healthc Mater* **6**, ID 1700121.
4. Mori H, Tsukada M (2000) New silk protein: modification of silk protein by gene engineering for production of biomaterials. *J Biotechnol* **74**, 95–103.
5. Meinel L, Hofmann S, Karageorgiou V, Kirker-Head C, McCool J, Gronowicz G, Zichner L, Langer R, et al (2005) The inflammatory responses to silk films *in vitro* and *in vivo*. *Biomaterials* **26**, 147–155.
6. Chithra P, Sajithlal GB, Chandrakasan G (1998) Influence of *Aloe vera* on the glycosaminoglycans in the matrix of healing dermal wounds in rats. *J Ethnopharmacol* **59**, 179–186.
7. Maenthaisong R, Chaiyakunapruk N, Niruntraporn S, Kongkaew C (2007) The efficacy of *Aloe vera* used for burn wound healing: A systematic review. *Burns* **33**, 713–718.
8. Femenia A, Sánchez ES, Simal S, Rosselló C (1999) Compositional features of polysaccharides from *Aloe vera* (*Aloe barbadensis* Miller) plant tissues. *Carbohydr Polym* **39**, 109–117.
9. Sahu PK, Giri DD, Singh R, Pandey P, Gupta S, Shrivastava AK, Kumar A, Pandey KD (2013) Therapeutic and medicinal uses of *Aloe vera*: A Review. *Pharmacol Pharm* **4**, 599–610.
10. Sanders ER (2012) Aseptic laboratory techniques: plating methods. *J Vis Exp* **63**, e3064.
11. Pinto Bi, Cruz ND, Lujan OR, Propper CR, Kellar RS (2019) *In vitro* scratch assay to demonstrate effects of arsenic on skin cell migration. *J Vis Exp* **144**, e58838.
12. He S, Shi D, Han Z, Dong Z, Xie Y, Zhang F, Zeng W, Yi Q (2019) Heparinized silk fibroin hydrogels loading FGF1 promote the wound healing in rats with full-thickness skin excision. *Biomed Eng Online* **18**, ID 97.
13. Monsuur HN, Boink MA, Weijers EM, Roffel S, Breetveld M, Gefen A, Broek LJ, Gibbs S (2016) Methods to study differences in cell mobility during skin wound healing *in vitro*. *J Biomech* **49**, 1381–1387.
14. Zhong J, Ma M, Li W, Zhou J, Yan Z, He D (2014) Self-assembly of regenerated silk fibroin from random coil nanostructures to antiparallel β-sheet nanostructures. *Biopolymers* **101**, 1181–1192.
15. Altman GH, Diaz F, Jakuba C, Calabro T, Horan RL, Chen J, Lu H, Richmond J, et al (2003) Silk-based biomaterials. *Biomaterials* **24**, 401–416.
16. Esua MF, Rauwald J-W (2006) Novel bioactive maloyl glucans from *Aloe vera* gel: Isolation, structure elucidation and *in vitro* bioassays. *Carb Res* **341**, 355–364.
17. Kumar K, Bhowmik D, Bhattacharjee C, Biswajit (2010)

Aloe vera: a potential herb and its medicinal importance. *J Chem Pharm Res* **2**, 21–29.
18. Das S, Mishra B, Gill K, Ashraf MS, Singh AK, Sinha M, Sharma S, Xess I, et al (2011) Isolation and characterization of novel protein with anti-fungal and anti-inflammatory properties from *Aloe vera* leaf gel. *Int J Biol Macromol* **48**, 38–43.
19. Koike T, Beppu H, Kuzuya H, Maruta K, Shimpo K, Suzuki M, Titani K, Fujita K (1995) A 35 kDa mannose-binding lectin with hemagglutinating and mitogenic activities from "Kidachi Aloe" (*Aloe arborescens Miller var. natalensis Berger*). *J Biochem* **118**, 1205–1210.
20. Fairand BP (2001) *Radiation Sterilization for Health Care Products. X-Ray, Gamma, and Electron Beam*, 1st edn, CRC Press, Boca Raton, Florida, USA.
21. Aquino K (2012) *Sterilization by Gamma Irradiation, Gamma Radiation*, IntechOpen Limited, London, UK.
22. AlZahrani K, Al-Sewaidan HA (2017) Nanostructural changes in the cell membrane of gamma-irradiated red blood cells. *Indian J Hematol Blood Transfus* **33**, 109–115.
23. Grieb TA, Forng R-Y, Stafford RE, Lin J, Almeida J, Bogdansky S, Ronholdt C, Drohan WN, et al (2005) Effective use of optimized, high-dose (50 kGy) gamma irradiation for pathogen inactivation of human bone allografts. *Biomaterials* **26**, 2033–2042.
24. Araújo ES, Khoury HJ, Silveira SV (1998) Effects of gamma-irradiation on some properties of durolon polycarbonate. *Radiat Phys Chem* **53**, 79–84.
25. Khan S, Villalobos MA, Choron RL, Chang S, Brown SA, Carpenter JP, Tulenko TN, Zhang P (2017) Fibroblast growth factor and vascular endothelial growth factor play a critical role in endotheliogenesis from human adipose-derived stem cells. *J Vasc Surg* **65**, 1483–1492.
26. Ferrara N (2000) VEGF: an update on biological and therapeutic aspects. *Curr Opin Biotechnol* **11**, 617–624.
27. Mandal BB, Kundu SC (2009) Cell proliferation and migration in silk fibroin 3D scaffolds. *Biomaterials* **30**, 2956–2965.
28. Teplicki E, Ma Q, Castillo DE, Zarei M, Hustad AP, Chen J, Li J (2018) The effects of *Aloe vera* on wound healing in cell proliferation, migration, and viability. *Wounds* **30**, 263–268.
29. Hengst L, Nigg EA (2006) Cell cycle: Overview. In: *Encyclopedic Reference of Genomics and Proteomics in Molecular Medicine*, Springer, Berlin, Heidelberg, pp 228–233.
30. Wei X, Guo W, Zou C-H, Fu T-T, Li X-Y, Zhu M, Qi J-H, Song J, et al (2015) Acemannan accelerates cell proliferation and skin wound healing through AKT/mTOR signaling pathway. *J Dermatol Sci* **79**, 101–109.
31. Bainbridge P (2013) Wound healing and the role of fibroblasts. *J Wound Care* **22**, 407–408, 410–412.
32. Yang VW (2012) Chapter 15: The cell cycle. In: Johnson LR, et al (eds) *Physiology of the Gastrointestinal Tract*, 5th edn, Academic Press, Boston, pp 451–471.
33. Kodama A, Lechler T, Fuchs E (2004) Coordinating cytoskeletal tracks to polarize cellular movements. *J Cell Biol* **167**, 203–207.
34. Harishkumar M, Masatoshi Y, Hiroshi S, Tsuyomu I, Masugi M (2013) Revealing the mechanism of *in vitro* wound healing properties of *Citrus tamurana* extract. *Biomed Res Int* **2013**, ID 963457.
35. Zhang S-L, Li B-L, Li W, Lu M, Ni L-Y, Ma H-L, Meng Q-G (2018) The Effects of ludartin on cell proliferation, cell migration, cell cycle arrest and apoptosis are associated with upregulation of p21WAF1 in Saos-2 osteosarcoma cells *in vitro*. *Med Sci Monit* **16**, 4926–4933.
36. Lamers ML, Almeida ME, Vicente-Manzanares M, Horwitz AF, Santos MF (2011) High glucose-mediated oxidative stress impairs cell migration. *PLoS One* **6**, ID e22865.
37. Desta T, Li J, Chino T, Graves DT (2010) Altered fibroblast proliferation and apoptosis in diabetic gingival wounds. *J Dent Res* **89**, 609–614.